Chapter 8
Equivalent Sources Using HELS

In an effort to reduce the overall measurement points associated with BEM-based NAH, Jeon and Ih [108] explore the use of an equivalent source method where the field acoustic pressures are regenerated by point sources distributed inside the real source surface. To this end, Jeon and Ih reformulate the HELS formulations by expanding the spherical Hankel functions and spherical harmonics with respect to multiple points distributed in the interior region of the source surface. Contributions from all equivalent sources are determined by matching the assumed-form solution to the boundary conditions specified on the source surface [109–111] or to the acoustic pressures on the hologram surface [13, 112–118]. The equivalent sources locations can be optimized by using either the natural algorithm [119] or EfI method [120]. The optimal number of expansion terms is obtained by using a spatial filter and regularization scheme. Once the expansion coefficients are specified, the field acoustic pressures are regenerated and taken as the input data to BEM codes, just like CHELS algorithms. In this way, the overall measurement points are greatly reduced.

All the aforementioned equivalent sources methods rely on a distribution of the monopole sources inside the actual source surface. This chapter presents a more effective equivalent sources by expanding the acoustic pressure field in terms of multipoles [121], which for whatever reasons have escaped the attention of researchers.

We have learned that HELS utilizes an expansion of the spherical waves to approximate the acoustic field generated by an arbitrary source. Similar expansions have been previously utilized to predict acoustic scattering and radiation: the Rayleigh series as discussed in Sect. 4.1, the point-matching method, and least-squares approximation method, which were collectively referred to as Rayleigh methods by some authors [122, 123]. Other expansions that employ outgoing spherical waves that satisfy the Helmholtz equation and Sommerfeld radiation condition to approximate an acoustic field include the localized spherical waves (LSW) [124], distributed spherical waves (DSW) [125], and distributed point sources (DPS) [126]. These expansions are collectively known as the discrete

S.F. Wu, *The Helmholtz Equation Least Squares Method*, Modern Acoustics and Signal Processing, DOI 10.1007/978-1-4939-1640-5_8

sources methods [127]. In Chapter 8 we discuss the discrete sources methods and how to combine them with the HELS formulations to reconstruct the acoustic field generated by an arbitrary source.

8.1 Localized Spherical Waves

LSW was employed to approximate the Green's function included in the Helmholtz integral formulation to predict acoustic radiation [125],

$$\left.\begin{matrix} u\left(\vec{x};\omega\right) \\ 0 \end{matrix}\right\} = \iint\limits_S \left[u\left(\vec{y};\omega\right) \frac{\partial G\left(\vec{x}|\vec{y};\omega\right)}{\partial \mathrm{n}\left(\vec{y}\right)} - \frac{\partial u\left(\vec{y};\omega\right)}{\partial \mathrm{n}\left(\vec{y}\right)} G\left(\vec{x}|\vec{y};\omega\right) \right] dS, \quad \begin{cases} \vec{x} \in \Omega_s \\ \vec{x} \in \Omega_i \end{cases}, \tag{8.1}$$

where Ω_s indicates the exterior region bounded by the source surface S and the sphere at infinity, and Ω_i implies the interior region inside the source surface S. In Eq. (8.1) the original format is followed as much as possible.

In an attempt to estimate the acoustic field $u\left(\vec{x};\omega\right)$, Doicu et al. [125] examined the systems of discrete sources as complete systems of functions. They found that there is a close relation between the properties of the acoustic field generated by discrete sources and the structure of their support. For example, a point structure corresponds to the LSW functions. Similarly, a straight line support parallels with the DSW functions, and a surface support is equivalent to the DPS.

Accordingly, if the acoustic field can be approximated by a point structure, LSW functions form a set of characteristic solutions to the Helmholtz equation in the spherical coordinates, which are given by

$$\begin{aligned} u_{mn}\left(\vec{x};\omega\right) &= h_n^{(1)}(kr) P_n^{|m|}(\cos\theta) \mathrm{e}^{jm\phi}, \quad n = 0, 1, 2, \ldots, \infty; \\ & m = -n \text{ to } +n. \end{aligned} \tag{8.2}$$

Using LSW, the Green's function in Eq. (8.1) is expressible as

$$G\left(\vec{x}|\vec{y};\omega\right) = \frac{jk}{\pi} \sum_{n=0}^{\infty} \sum_{m=-n}^{n} E_{mn} u_{mn}\left(\vec{x}\right) u_{-mn}\left(\vec{y}\right), \tag{8.3}$$

where u_{mn} and u_{-mn} are defined in Eq. (8.2) and the expansion coefficients E_{mn} are given by

$$E_{mn} = \frac{(2n+1)}{4} \frac{(n-|m|)!}{(n+|m|)!}. \tag{8.4}$$

The following theorem has been proven by Doicu et al. [125]

First of all, let us define some terminologies. Let S be the boundary of a bounded domain $D_i \subset \mathbf{R}^3$, namely, a bounded, open, and connected subset of three-dimensional space $\mathbf{R}^3$. We say that the surface S is of class C^2 if for each point $\vec{x} \in S$ there exists a neighborhood $V_{\vec{x}}$ of $\vec{x}$ such that the intersection $V_{\vec{x}} \cap S$ can be mapped bijectively onto a domain $U \subset \mathbf{R}^2$, and this mapping is twice continuously differentiable. We express this property by saying that D_i is of class C^2.

Theorem 8.1 *Let S be a closed surface of class C^2 and $\vec{n}$ denote the unit outward normal to S. Then the system $u_{mn}\left(\vec{x};\omega\right) = h_n^{(1)}(kr)P_n^{|M|}(\cos\theta)\mathrm{e}^{im\phi}$, $n = 0, 1, 2, \ldots, \infty$; $m = -n$ to $+n$, is complete in $L^2(S)$.*

As discussed in Sect. 4.1, an infinite series is not suitable for our applications, which is especially true for reconstructing the acoustic field generated by an arbitrary source. However, we can adopt the concept of LSW and try instead the following finite expansion:

$$\hat{p}\,(r,\theta,\phi;\omega) = \sum_{n=0}^{N} \sum_{m=-n}^{n} a_{nm} h_n^{(1)}(kr) P_n^{|m|}(\cos\theta)\mathrm{e}^{im\phi}, \tag{8.5}$$

where a_{nm} represent the expansion coefficients, N is the order of expansion, and the total number of expansion terms is $J = (N+1)^2$. Note that there is a subtle difference between LSW and HELS in that the former uses $P_n^{|m|}(\cos\theta)\mathrm{e}^{im\phi}$ in the expansion, whereas the latter uses the standard spherical harmonics $P_n^m(\cos\theta)\mathrm{e}^{im\phi}$ in the expansion. From Eq. (2.16) we see that $P_n^{|m|}(\cos\theta)\mathrm{e}^{im\phi}$ differs from $P_n^m(\cos\theta)\mathrm{e}^{im\phi}$ by a constant $(-1)^m$, which may be absorbed by the expansion coefficients a_{nm}. Thus Eq. (8.5) is in effect the same as the HELS expansion. Since LSW corresponds to a point source, the corresponding auxiliary source is located at the origin of the coordinate system.

8.2 Distributed Spherical Waves

In [125] Doicu et al. considered the system of DSW functions, which form a set of radiating solutions to the Helmholtz equation (4.6). These DSW functions are given by

$$u_{m\left|m\right|}\left(\vec{x}-z_n\vec{e}_z\right)=h_{|m|}^{(1)}(kr_n)P_{|m|}^{|m|}(\cos\theta)\mathrm{e}^{jm\phi}, \tag{8.6}$$

where the discrete sources are distributed along a segment of the z-axis at a radius with respect to the origin, which are expressible in the spherical coordinates as $(r_n, \theta_n, \phi_n), r_n=\sqrt{x^2+y^2+(z-z_n)^2}$, and $n=1, 2, \ldots, \infty$, and $m \in \Xi$, where Ξ is the support of the discrete sources that consist of the origin of the coordinate system.

The following theorem has been proven by Doicu et al. [125]

Theorem 8.2 *Consider the bounded sequence $(z_n) \subset \Xi$, where Ξ is a segment of the z-axis. Assume that S is a surface of class C^2 enclosing Ξ. Replace in Theorem 8.1 the LSW functions $u_{mn}\left(\vec{x};\omega\right)$ by $u_{m\left|m\right|}\left(\vec{x}-z_n\vec{e}_z\right)=h_{|m|}^{(1)}(kr_n)P_{|m|}^{|m|}(\cos\theta)\mathrm{e}^{jm\phi}$, $n=1, 2, \ldots, \infty$, and $m \in \Xi$. Then the resulting systems of functions are complete in $L^2(S)$.*

These theorems state that Eq. (8.6) may be utilized to describe the radiated acoustic field completely. Once again, we adopt the concept of DSW and utilize instead a finite expansion,

$$\hat{p}\left(\vec{x};\omega\right)=\sum_{n=1}^{n_{\max}}\sum_{m=-m_{\max}}^{m_{\max}}b_{mn}h_{|m|}^{(1)}(kr_n)P_{|m|}^{|m|}(\cos\theta_n)\mathrm{e}^{jm\phi}, \tag{8.7}$$

where b_{mn} are the expansion coefficients, $n_{\max}$ is the number of auxiliary sources and $m_{\max}$ is the order of expansion, and the total number of expansion terms is $J=n_{\max}(2m_{\max}+1)$. For simplicity, we consider the case where the auxiliary sources are distributed along a segment of the z-axis with its center at the origin of the coordinate system,

$$z_n=z_0\cos\beta_n, \tag{8.8}$$

where $n=1, 2, \ldots, n_{\max}$, z_0 is chosen such that all auxiliary sources are inside Ω_s (some of them can be close to the boundary surface S), and β_n are given by

$$\beta_n=\frac{\pi}{2n_{\max}}+\frac{\pi(n-1)}{n_{\max}}. \tag{8.9}$$

The z_nth auxiliary source is at $\vec{x}-z_n\vec{e}_z$, which is expressible in the cylindrical coordinates as

$$r_n=\sqrt{r^2\sin^2\theta+(r^2\cos^2\theta-z_n)^2}, \tag{8.10}$$

$$\sin\theta_n = \frac{r\sin\theta}{r_n}, \tag{8.11}$$

$$r = \sqrt{x^2 + y^2}. \tag{8.12}$$

8.3 Distributed Point Sources

DPS is known as fundamental solutions to the Helmholtz equation, which are given by

$$\varphi_n\left(\vec{x}\middle|\vec{x}_n;\omega\right) = G\left(\vec{x}\middle|\vec{x}_n;\omega\right), \tag{8.13}$$

where $n = 1, 2, \ldots, \infty$, and $\left\{\vec{x}_n\right\}^{\mathrm{T}}_{1\times\infty}$ is a set of discrete point sources distributed on a closed surface S of class C^2. Suppose that $\left\{\varphi_n^-\left(\vec{x}\middle|\vec{x}_n;\omega\right)\right\}^{\mathrm{T}}_{1\times\infty}$ denote the fundamental solutions with point sources $\left\{\vec{x}_n^-\right\}^{\mathrm{T}}_{1\times\infty}$ distributed on the interior surface S^-, and $\left\{\varphi_n^+\left(\vec{x}\middle|\vec{x}_n;\omega\right)\right\}^{\mathrm{T}}_{1\times\infty}$ indicate those with the sources $\left\{\vec{x}_n^+\right\}^{\mathrm{T}}_{1\times\infty}$ distributed on the exterior surface S^+. The completeness of DPS as given by Eq. (8.13) is provided by the following theorem, which has been proven by Doicu et al. [125]

Theorem 8.3 *Consider Ω_i a bounded domain of class C^2. Let the set $\left\{\vec{x}_n^-\right\}^{\mathrm{T}}_{1\times\infty}$ be dense on a surface S^- enclosed in Ω_i and let set $\left\{\vec{x}_n^+\right\}^{\mathrm{T}}_{1\times\infty}$ be dense on a surface S^+ enclosing Ω_i. Assume that k is not an eigenvalue of the boundary value problem for the interior region Ω_i. Replace in Theorem 8.1 the radiating spherical wave functions $u_{mn}\left(\vec{x};\omega\right) = h_n^{(1)}(kr)P_n^{|m|}(\cos\theta)\mathrm{e}^{jm\phi}$, $n = 0,\ 1,\ 2,\ \ldots,\ \infty$, and $m = -n$ to n by the functions $\left\{\varphi_n^-\left(\vec{x}\middle|\vec{x}_n;\omega\right)\right\}^{\mathrm{T}}_{1\times\infty}$ $n = 0,\ 1,\ \ldots,\ \infty$, and the regular spherical wave functions $u_{mn}\left(\vec{x};\omega\right) = j_n^{(1)}(kr)P_n^{|m|}(\cos\theta)\mathrm{e}^{jm\phi}$, where $j_n^{(1)}(kr)$ is the spherical Bessel functions of the first kind, $n = 0,\ 1,\ 2,\ \ldots,\ \infty$, and $m = -n$ to n by $\left\{\varphi_n^+\left(\vec{x}\middle|\vec{x}_n;\omega\right)\right\}^{\mathrm{T}}_{1\times\infty}$ $n = 0, 1, \ldots, \infty$. Then, the resulting systems of functions are complete in $L^2(S)$.*

We adopt the DPS concept in reconstruction, but instead use a finite expansion,

$$\hat{p}\left(\vec{x};\omega\right) = \sum_{n=1}^{n_{\max}} c_n h_0^{(1)}\left(k\left|\vec{x} - \vec{x}_n\right|\right), \tag{8.14}$$

where c_n are the expansion coefficients, $n_{\max}$ is the number of point sources, and

$$h_0^{(1)}\left(k\left|\vec{x}-\vec{x}_j\right|\right)=\frac{\mathrm{e}^{ik\left|\vec{x}-\vec{x}_j\right|}}{\left|\vec{x}-\vec{x}_j\right|}, \tag{8.15}$$

is the fundamental solution (or the free-space Green's function) to the Helmholtz equation. Hence the auxiliary sources in DPS are a set of point sources distributed on a smooth surface S^- inside Ω, but close to the boundary surface S.

Note that DPS formulation (8.14) is the same as those of the so-called equivalent source methods [108−119], and LSW is the same as HELS. Here LSW, DSW, and DPS will be adopted in the HELS expansion to reconstruct the acoustic field generated by a vibrating object in free space. Their results will be validated against the benchmark values and their performances be examined.

8.4 Regularization for LSW, DSW, and DPS Expansions

It is well known that the rate of convergence of any expansion depends on the complexity of the source boundary and frequency [124, 128–130]. Although reconstruction of acoustic quantities may be done by HELS at any frequencies, the accuracy in reconstruction may deteriorate with an increase in the frequency. This is because at high frequencies, SNR is usually very low such that the high-order terms in the HELS expansion may be contaminated by background noise. To avoid distortions in reconstruction due to noise contamination, we must truncate the HELS expansion by eliminating the high-order terms. However, the high-order terms are critical in depicting the details of acoustic quantities at high frequencies and an omission of these terms will make it impossible to obtain the details in reconstruction. It is emphasized that this high-frequency difficulty exists in other methods, for example, BEM, whose performance deteriorates greatly at high frequencies.

Despite the fact that discrete sources methods have been extensively studied in the forward problems such as scattering and prediction of acoustic fields, they have not been tested in backward problems such as reconstruction of acoustic fields, with the exception of HELS. Since the matrix involved in HELS is relatively small, it is possible to utilize a direct regularization method such as TR. For a problem that involves a large matrix, for example, in three-dimensional simulations, an iterative regularization method may be a better alternative.

Success in regularization depends to a large extent on choice of regularization parameter. Based on the type of information available on a targeted solution, the parameter-choice methods (PCM) are classified as a priori, which is independent of the actual data, and a posteriori, which is dependent on the actual data [131]. The former includes heuristic or error-free [132] methods that do not require the knowledge of the noise level in the input data and seek to predict this information from actual data. Note that for an infinite-dimensional compact operator, error-free

PCM may fail to yield a convergent regularization parameter, namely, to provide a regularized solution that will converge to the exact solution as the noise level tends to zero [133].

In practice, there is always noise in the input data and its level is unknown a priori. Hence we must resort to the error-free PCM, even though it may occasionally fail to yield a convergent regularization parameter. Of course, if noise level can be estimated a priori, we can use Morozov's discrepancy principle [106, 134] to determine the correct regularization parameter and get satisfactory reconstruction. Alternatively, we can impose constraints on the norm of a regularized solution as suggested by Isakov and Wu [74] to find a convergent regularization parameter. The trouble is that the right constraint for the norm of the exact solution is hard to find.

Our objective is to examine the effects of different expansions on resultant reconstruction and, more importantly, to identify the expansion that can produce the most accurate and efficient reconstruction.

Specifically, we consider three expansions: LSW, DSW, and DPS in HELS to reconstruct the acoustic pressure radiated from an arbitrary source in free space. In particular, we use TR, MTR, and damped singular value decomposition (DSVD) in regularization scheme with its regularization parameter determined by an error-free PCM such as GCV, L-curve criterion, and quasi-optimality criterion (QOC) [135]. Reconstructed acoustic quantities are validated with respect to the benchmark data measured at the same locations as the reconstruction points.

The L-curve criterion [136] relies on a parametric plot of the norm of a regularized solution versus the residual norm in a log–log scale with respect to the regularization parameter. The corner of an L-curve (which is defined as the point of maximum curvature) separates the horizontal part (where regularization errors dominate) from the vertical part (where perturbation errors dominate), and represents a balance between the regularization and perturbation errors.

8.5 Performances of LSW, DSW, and DPS Expansions

Here we examine the performances of HELS through LSW (8.5), DSW (8.7), and DPS (8.14) expansions to reconstruct the acoustic pressures generated by a JBL® speaker that consists of a woofer, mid-ranger, and tweeter inside a fully anechoic chamber (see Fig. 8.1). In particular, we examine the convergence rates of these expansions and condition numbers of the corresponding transfer matrices. The faster the convergence rates and the smaller the condition numbers are, the more efficient the numerical computations and the more accurate the HELS solutions become.

In experiments the speaker was driven by an HP 8904A Multi-Function Synthesizer DC-600 kHz and a McIntosh MC352 Power Amplifier to produce white noise. The acoustic pressures were measured by an array of 56 PCB T130D21 free-field

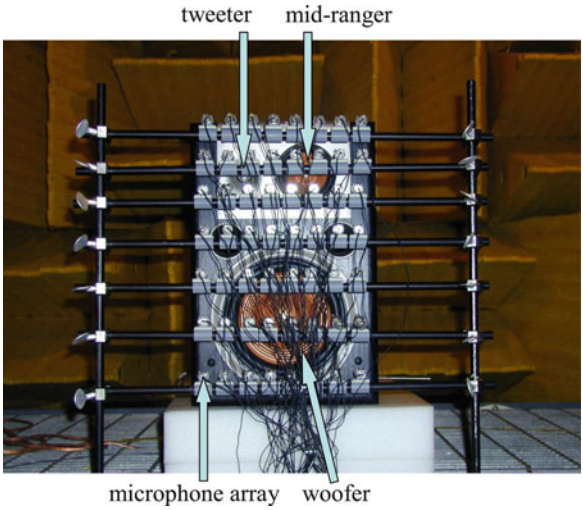

Fig. 8.1 Test setup for reconstructing the acoustic pressure emitted from a JBL® speaker that consists of a woofer, mid-ranger, and tweeter inside a fully anechoic chamber. Input data were collected by an array of microphones

microphones (see Fig. 8.1). The input data were sent to a personal computer through the Larson Davis digital Sensor System Model 100 for analog to digital conversion.

Test procedures were as follows. First, the radiated acoustic pressures were measured on a planar surface Γ at 1 cm clearance in front of the speaker. These data were taken as input to HELS using LSW, DSW, and DPS expansions, respectively, to reconstruct the acoustic pressures on a surface S at 0.5 cm clearance in front of the speaker up to 3,275 Hz (see Fig. 8.2). The reason for selecting this surface S was that there was no way of measuring the acoustic pressures on the speaker membrane directly.

Next, the acoustic pressures on this surface S were measured using the same microphone array, and these benchmark values were compared with the reconstructed acoustic pressures at the same locations. The measurement points on Γ and S were equidistant. The origin of the coordinate system was set at the geometric center of the speaker. In particular, the auxiliary source for LSW was placed at the geometric center of the speaker, those for DSW were distributed along a vertical axis between the front surface and center of the speaker box, and those for DPS were distributed on a plane next to the front surface of the speaker (see Fig. 8.2).

For simplicity without loss of generality, we consider reconstructing the acoustic pressure in front of the speaker. The characteristic dimension was $a = \sqrt{(0.28/2)^2 + (0.42/2)^2} = 0.28$ m. So for the highest frequency of 3,275 Hz, the maximum dimensionless frequency was $ka_{\max} \approx 16.6$.

Since we were only interested in reconstructing the acoustic pressure, it was acceptable to gauge the number of expansion terms with respect to the maximum dimensionless frequency $ka_{\max}$. From [37] we learn that the total number of expansion terms for LSW is $J = (N+1)^2$; here, N is the order of expansion. In general, we may set $N = ka_{\max} \approx 17$. So $J = 324$. Accordingly, we need at least

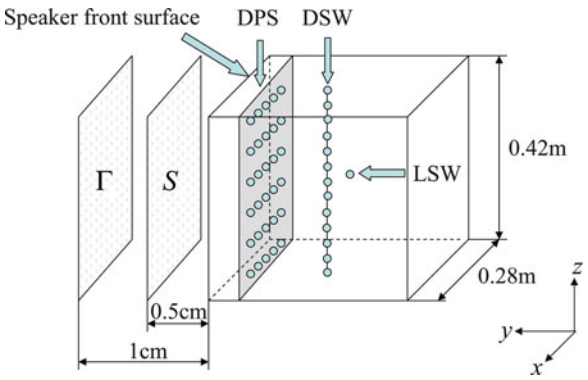

Fig. 8.2 Schematic of the locations of the auxiliary sources for LSW, DSW, and DPS expansions inside the JBL® speaker. The measurement surfaces Γ and S were in front of the speaker at, respectively, 1 and 0.5 cm away

324 measurement points on Γ to cover the specified frequency range. In practice, we may have to truncate the expansion to reduce distortion due to a low SNR at high frequencies. In this experiment, we set $N = 9$, so $J = 100$.

The number of expansion terms in DSW is $J = n_{\max}(2m_{\max} + 1)$, where $n_{\max}$ is the number of auxiliary sources and $m_{\max}$ is the order of expansion, which is smaller than N in LSW. There are no known theories or methodologies that we can use to estimate the optimum values of $n_{\max}$ and $m_{\max}$ for arbitrarily shaped sources. In general, the values of $n_{\max}$ and $m_{\max}$ depend on the complexities of source geometry and the highest frequency of interest. To achieve the best results, it is a good idea to set distances among neighboring auxiliary sources to be less than one wavelength of the highest frequency of interest and distribute the auxiliary sources evenly on a conformal surface inside the source boundary.

For example, the front surface of the speaker is of dimensions 0.28×0.42 m^2, the highest frequency is $f_{\max} = 3{,}275$ Hz, and the acoustic wavelength is $\lambda_{\min} = c/f_{\max} \approx 0.104$ m. Therefore, the estimated number of auxiliary sources for DSW is $n_{\max} = (0.28/0.104) \times (0.42/0.104) \approx 11$. Since the speaker in free space is often modeled as a dipole, we set the highest order of expansion for DSW at $m_{\max} = 4$. Accordingly, the number of expansion terms is $J = 99$. Therefore we need to take 100 measurement points of the acoustic pressures on Γ to guarantee satisfactory reconstruction of the acoustic pressures in the specified frequency range.

In DPS, the auxiliary sources are distributed uniformly on a surface conformal to a source boundary from the inside. However, the optimal number and locations of the auxiliary sources are unknown a priori, whose determination is a topic of research by itself and will not be considered here. Since the front surface of the speaker is planar, it is sufficient to distribute the auxiliary sources on a plane with $J = n_x \times n_z$, where n_x and n_z are, respectively, the numbers of sources in the x- and z-axis directions. Here we set $n_x = 10$ and $n_z = 10$, so $J = 100$.

In this experiment 112 measurement points of the acoustic pressures were taken on Γ and S, respectively, which were enough for LSW, DSW, and DPS expansions.

It is emphasized that the number of measurement points is not as critical as it seems. The controlling factor is SNR. If SNR is low, there is no way of obtaining good reconstruction because the critical near-field information will be buried in

background noise. Accordingly, the number of expansion terms must be significantly reduced to avoid distortion in reconstructed images. Under this condition, the reconstructed results will not be good no matter how many measurement points are taken.

8.6 Locations of the Auxiliary Sources

Selection of the auxiliary source locations can be crucial to the success of reconstruction. Although there is no known theory that can depict exactly the interrelationship between locations of auxiliary sources and rate of convergence of resultant expansion and reconstruction accuracy, the following guideline is clear: the analytic continuation of solution to the Helmholtz equation requires that the surface on which auxiliary sources are distributed must enclose all singularities of an acoustic field.

However the singularities for a given acoustic field are unknown a priori. To gain a good understanding of the singularities locations, we start from an arbitrarily selected auxiliary surface, and measure the acoustic pressures on surfaces Γ and S, respectively. Next, we substitute the data measured on Γ to reconstruct the acoustic pressures on S and calculate the mean relative errors in reconstruction with respect to the benchmark data on S. Finally, we move the auxiliary surface to a different location, and repeat these processes again. Note that there is no need to remeasure the acoustic pressures on S. This iteration is continued until the mean relative errors in reconstruction are minimized, and the corresponding locations of the auxiliary sources are optimized for a given frequency and a set of measurements.

It is emphasized that in practice we only measure the acoustic pressures on the surface Γ. The reason for taking an additional set of measurements on S is to develop a guideline for selecting the optimal location of an auxiliary surface for a specific expansion function. Needless to say, the impact of the auxiliary source locations for different expansions is different. Hence, by taking an independent set of measurements on S, we can validate the reconstructed acoustic pressures, find the optimal location of an auxiliary surface for a given expansion, and study the sensitivity of the auxiliary surface on the reconstruction accuracy using this expansion.

Figure 8.3 depicts the mean relative errors in reconstructing acoustic pressures on S using LSW, DSW, and DPS, respectively, with respect to the auxiliary sources distributed on a plane at $y = -y_0$, where y_0 varies from -0.7 to 0.13 m, for a fixed frequency of 1,690 Hz. Results show that DSW is relatively insensitive to the auxiliary source locations as compared to LSW and DPS are. At the optimum auxiliary surfaces, LSW and DSW can yield nearly the same level of accuracy in reconstruction, whereas DPS produces a slightly lower accuracy in reconstruction.

It is interesting to observe that LSW places its optimum location of the auxiliary surface near the origin of the coordinate system, DSW moves its optimum auxiliary surface slightly away from the origin of the coordinate system toward the front

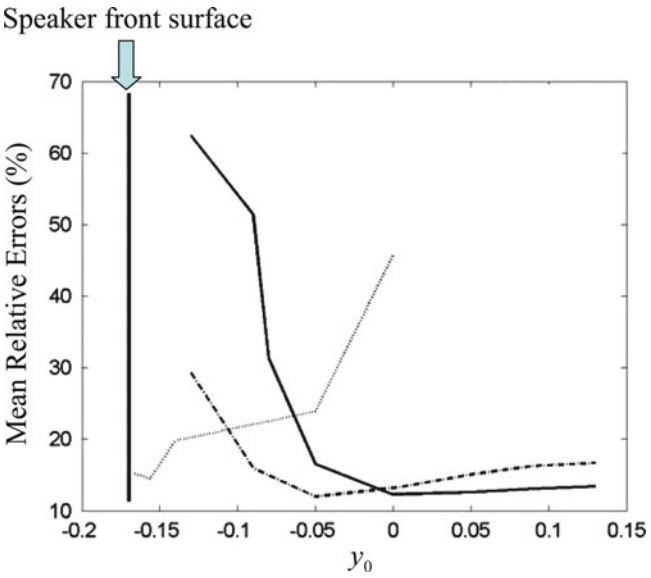

Fig. 8.3 Comparison of the auxiliary surface locations at 1,690 Hz. *Continuous line*: for LSW; *broken line*: DSW; and *dotted line*: DPS

surface of the speaker, and DPS places its optimum auxiliary surface right behind the front surface of the speaker system.

Note that the standoff distance and frequency can also affect the reconstruction accuracy. However, their effects are negligible compared to those of the auxiliary source surface location. So we focus on the determination of optimal locations of auxiliary source surfaces by minimizing the mean relative errors in reconstruction with respect to the benchmark values measured on S.

8.7 Condition Number of the Transfer Matrices

Reconstruction of acoustic radiation from any source is an ill-posed problem. As a result, the transfer matrix in HELS may be ill conditioned. Ill conditioning of any matrix is measured by the 2-norm condition number defined as the ratio of the largest to smallest singular values of the matrix. This can be done prior to taking any measurements, if the frequency and measurement and reconstruction locations are specified. In many situations, if the condition number is in the order of $O(10^3)$ or higher, the matrix may be ill conditioned; if the condition number is in the order of $O(10^2)$ or lower, the matrix is more or less well conditioned. Regularization may be omitted if the transfer matrix is well conditioned, but must be implemented if the matrix is ill conditioned.

In our experiments, the condition numbers of the transfer matrices for a selected standoff distance and frequency were found to be: $O(10^1)$ for DSW, $O(10^2) \sim O(10^3)$ for LSW, and $O(10^5)$ for DPS. Therefore, for the same frequency and measurement and reconstruction locations, DSW offers the best-conditioned transfer matrix among all three expansions. This is expected because DSW uses a lower-order spherical Hankel function ($m_{\max} = 4$) than LSW does ($N = 9$). The small singular values are always associated with high-order expansion terms, and the condition number of a transfer matrix containing the high-order terms is much larger than that of a transfer matrix containing the low-order terms. The reason for DPS to produce an ill-conditioned transfer matrix may be attributed to the fact that the sound field produced by the present speaker system cannot be adequately described by a distribution of point sources because there are three speakers that emit sounds simultaneously. Consequently, the resultant transfer matrix in DPS becomes rank deficient and ill conditioned.

From the calculated condition numbers, we see that regularization is needed for DPS and LSW, but not needed for DSW. Since condition numbers are calculated before measurements are taken, no information on noise level in the input data is available. Consequently, we have to resort to an error-free PCM in regularization.

One of our objectives is to examine the performances of HELS using different expansions to reconstruct acoustic radiation from an arbitrary source. To this end, we first calculate the ideal regularization parameter by minimizing reconstruction errors with respect to the benchmark data on S. This process allows for assessing not only the reconstruction accuracy but also the impact of reducing the measurement number on reconstruction using various expansions. This latter is of great importance since in practice fewer measurement points mean bigger savings in time and costs.

8.8 Effect of Measurement Number

The effect of the number of measurement points on reconstruction accuracy is examined. Figures 8.4, 8.5, and 8.6 describe the mean relative errors in reconstructing the acoustic pressure through LSW, DSW, and DPS expansions, respectively, under different numbers of measurement points. Since the frequency range is relatively low, SNR is relatively high. So the more the measurements are taken, the higher the accuracy in regularized reconstruction becomes.

Note that regularization can significantly enhance the reconstruction accuracy, especially at higher frequencies. This is obvious in Figs. 8.4 and 8.6 since the transfer matrices for LSW and DPS are ill conditioned. However, the impact of regularization on reconstruction accuracy for DSW is not as drastic (see Fig. 8.5) because its transfer matrix is more or less well conditioned. Note that we have used ideal regularization parameters for all three expansions to maximize these effects. The calculated regularization parameters for LSW and DPS increased monotonically with frequency from 0.002 to 0.05, whereas that remained negligibly small at

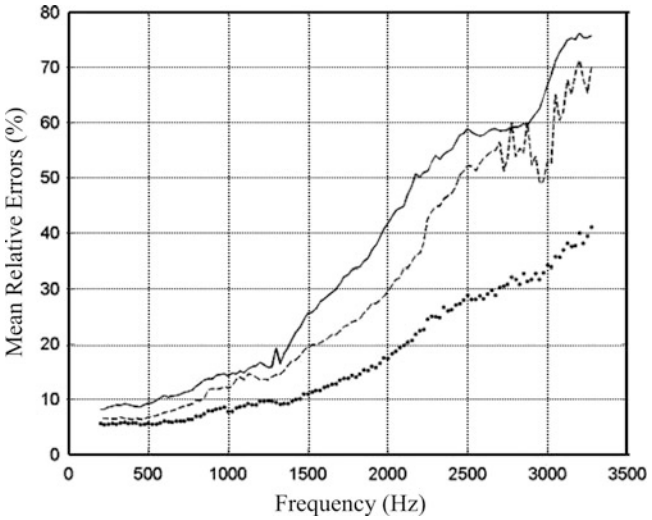

Fig. 8.4 Comparison of the mean relative errors in reconstructing the acoustic pressure by using LSW expansion. *Continuous line*: 56 measurement points with an ideal regularization parameter; *broken line*: 112 measurement points without using regularization; *dotted line*: 112 measurement points with an ideal regularization parameter

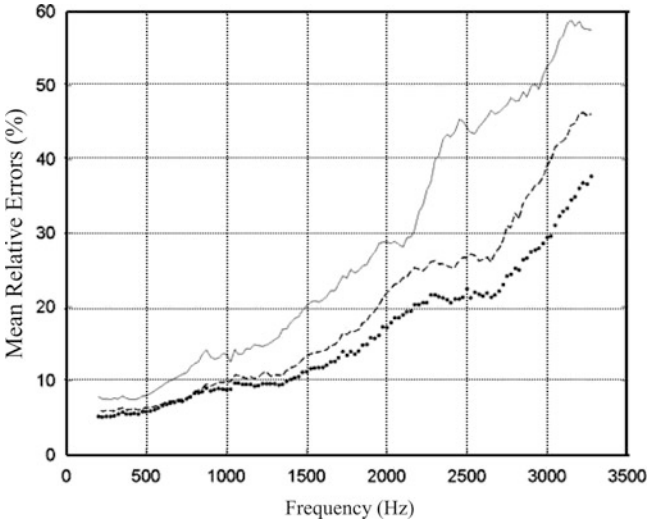

Fig. 8.5 Comparison of the mean relative errors in reconstructing the acoustic pressure by using DSW expansion. *Continuous line*: 56 measurement points with an ideal regularization parameter; *broken line*: 112 measurement points without using regularization; *dotted line*: 112 measurement points with an ideal regularization parameter

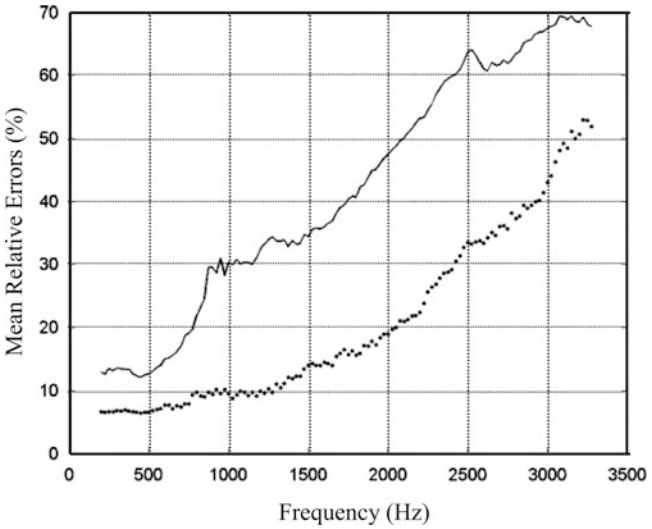

Fig. 8.6 Comparison of the mean relative errors in reconstructing the acoustic pressure by using DPS expansion. *Continuous line*: 56 measurement points with an ideal regularization parameter; *dotted line*: 112 measurement points with an ideal regularization parameter

0.0008 for DSW, which meant that there was almost no need for regularization in DSW within this frequency range.

Results demonstrate that even with an ideal regularization parameter, DPS failed to yield a compatible level of accuracy as compared to those of DSW and LSW under the same set of input data. Moreover, DPS is more sensitive to PCM than DSW and LSW are.

It is emphasized that for ill-conditioned transfer matrices, just increasing the numbers of measurement points and expansion terms in HELS without implementing regularization will only further distort reconstruction. This is seen in Fig. 8.6 using the DPS expansion. As the number of measurement points was doubled, the mean relative errors in reconstruction exceeded 200 % when no regularization was used (the corresponding curve was omitted in Fig. 8.6 for clarity). The reason for that was because the high-order terms in DPS expansion were contaminated by noise embedded in measured data, and these errors were significantly amplified as the acoustic pressures were projected back toward the source surface. When the transfer matrix is not highly ill conditioned, as in the case of LSW expansion, increasing the measurement number can improve reconstruction accuracy to certain frequency without regularization (see Fig. 8.4). If the transfer matrix is more or less well conditioned, as in the case of DSW expansion, increasing the number of measurement points allows for an increase in the number of expansion terms, which enhances the reconstruction accuracy even without regularization (see Fig. 8.5).

8.9 Choice of Regularization

In many engineering applications, the noise level embedded in the input data is unknown a priori. Thus we must rely on an error-free PCM in regularization. In this study, we want to find out if there exists an optimal regularization with an error-free PCM for each of DSW, LSW, and DPS expansions in HELS. To this end, we examine performances of all possible combinations of TR and its modification implemented by utilizing GCV and DSVD, together with various penalty functions with respect to pressure, normal velocity, or both, and error-free PCM such as GCV, L-curve, and QOC to select the best regularization parameter. Results show that for some expansions, it is possible to find the optimal regularization with an error-free PCM that can produce an almost ideal regularization parameter over a wide frequency range; but for other expansion such optimal combinations cannot be found. For brevity, we summarize the most important results here:

1. The optimal regularization for DSW is MTR implemented through DSVD, and the best regularization parameter can be provided by L-curve together with an energy norm as its penalty function.
2. The optimal regularization for LSW is TR implemented by GSVD with its regularization parameter determined by GCV using an energy norm as its penalty function. Depicted in Fig. 8.7 is the comparison of the mean relative errors in reconstruction using LSW and TR with its regularization parameter determined by different error-free PCMs. It is clear that the regularization parameter given by GCV is almost identical to the ideal value over the specified frequency range, that provided by L-curve is close to an ideal one, but those produced by QOC are way off the target. Figure 8.8 shows the regularization parameters given by GCV, L-curve, and QOC for TR in LSW versus the frequency. Results illustrate that GCV yields nearly the ideal regularization parameters, L-curve gives a regularization parameter close to the ideal one, but the regularization parameter provided by QOC is off by at least two orders of magnitude of an ideal value.
3. For DPS, it is not possible to find one regularization scheme that can produce satisfactory reconstruction over a wide frequency range. In fact, we must utilize different combinations of regularization, penalty function, and error-free PCM to select an optimal regularization parameter for different frequency.

Figure 8.9 summarizes the results of this investigation on determining optimal choices of regularization schemes for DSW, LSW, and DPS expansions in HELS. Comparing Fig. 8.9 with Figs. 8.4 and 8.5 demonstrates that using the optimal regularization schemes, for example, TR implemented by DSVD with its regularization parameter specified by L-curve for DSW, and TR with its regularization parameter determined by GCV for LSW, we can obtain the same level of reconstruction accuracy as that produced by an ideal regularization. When we only rely on a single regularization scheme, for example, TR and GCV for DPS, the mean relative reconstruction errors can be very large, especially at higher frequencies. This can be seen by comparing the mean relative errors in Fig. 8.9 with those in Fig. 8.5.

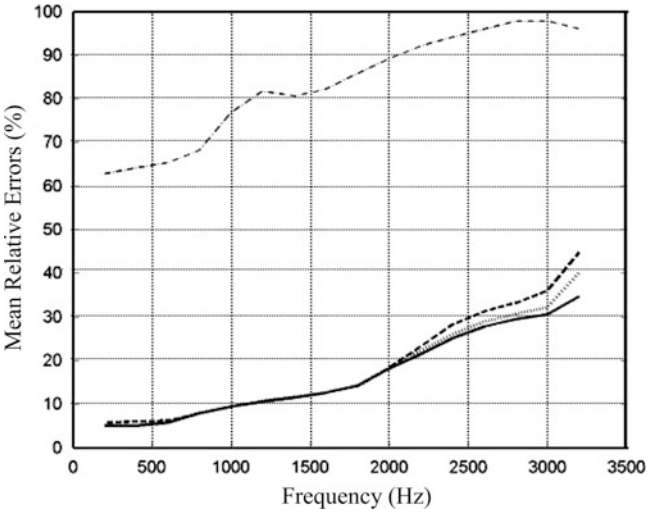

Fig. 8.7 Comparison of the mean relative errors in reconstructing the acoustic pressure by using LSW expansion in HELS with TR and various error-free PCM. *Broken line with dots*: QOC; *broken line*: L-curve; *dotted line*: GCV; *continuous line*: Ideal case

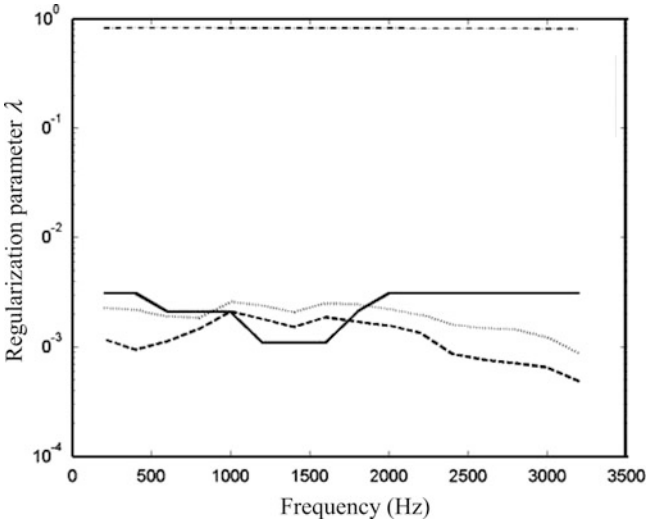

Fig. 8.8 Comparison of regularization parameters calculated by using various error-free PCMs for reconstructing the acoustic pressure using LSW in HELS. *Broken line with dots*: QOC; *broken line*: L-curve; *dotted line*: GCV; *continuous line*: Ideal case

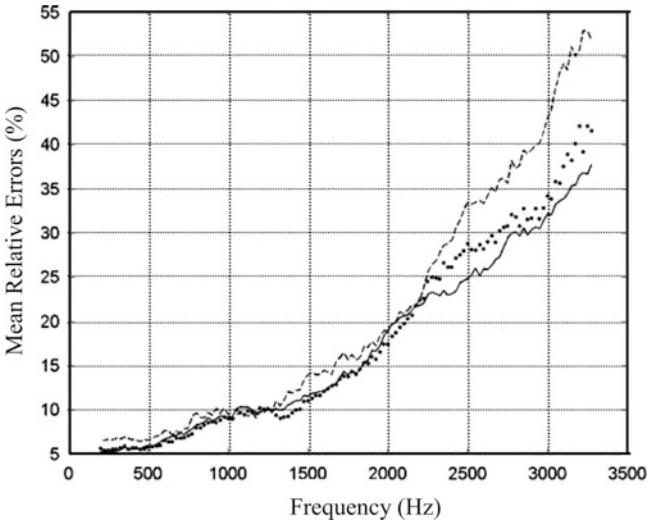

Fig. 8.9 Comparison of the mean relative errors in reconstructing the acoustic pressure using different expansions with regularization strategies. *Continuous line*: DSW using DSVD and L-curve; *dotted line*: LSW using TR and GCV; *broken line*: DPS using TR and GCV

It must be emphasized that there is no single regularization strategy that can yield the best reconstruction for all sources under all circumstances. For example, although TR and DSVD plus L-curve work well for DSW in the present case, it may not work well in a different scenario or in a different frequency range. The best regularization strategy is always case dependent. Also, we must keep in mind that an error-free PCM can fail to yield a convergent regularization parameter at all. On the other hand, it is always advantageous to take double-layer measurements whenever possible. These double-layer measurements can help us to device optimal regularization schemes and produce the best reconstruction of the acoustic quantities.

To summarize, results show that DSW leads to the best-conditioned transfer matrix, is the least sensitive to choices of auxiliary surface locations, and yields most satisfactory reconstruction over a wide frequency range. LSW is the second best choice of expansion for HELS, its transfer matrix can be weakly ill conditioned, and its optimal auxiliary source location can be close to the geometric center of a source. If the optimal location for the auxiliary source is selected, LSW can yield nearly the same level of accuracy in reconstruction as DSW does. Moreover, it is possible to improve the reconstruction accuracy in LSW by increasing the measurement points taken at very close range to the source surface, even without regularization. DPS gives a highly ill-conditioned transfer matrix and is very sensitive to the auxiliary surface location. The reason for that may be due to the fact that the acoustic pressure radiated from an arbitrary source may not be adequately described by a distribution of point sources. When DPS expansion is

used in HELS, it is necessary to implement regularization in order to obtain a convergent reconstruction.

The optimal regularization for DSW is MTR implemented through DSVD plus L-curve to determine the regularization parameter with an energy norm as its penalty function. The optimal regularization for LSW is TR implemented by DSVD plus GCV to determine its regularization parameter with an energy norm as its penalty function. There is no single optimal regularization scheme that can produce satisfactory reconstruction over a wide frequency range for DPS. In this case, different regularization schemes must be used at different frequencies in order to produce satisfactory reconstruction.

It is emphasized that it may not be possible to find the optimal regularization schemes for DSW and LSW that will work for all scenarios. In other words, there is no single regularization strategy that can guarantee good reconstruction for all sources under all conditions.

Finally, it is always a good idea to take double-layer measurements. Such measurements can help us to determine the optimal auxiliary surface location for particular expansion functions in HELS and to select the optimal regularization scheme that includes choosing penalty functions and error-free PCMs to yield the best regularization parameter.

Problems

8.1. What is LSW? What does it attempt to do? What are the differences between LSW and the Helmholtz integral formulation?
8.2. What are the differences between LSW and the HELS method? Will LSW suffer from the same difficulties as those of the Rayleigh hypotheses for a corrugated surface?
8.3. What is DSW? What does it attempt to do? What are the differences between DSW and the original HELS method?
8.4. What are the differences between DSW and the HELS method using the DSW expansion?
8.5. Will DSW have the same difficulties as those of the Rayleigh hypotheses for a corrugated surface? Will the HELS method using DSW expansion have the same difficulties as DSW for a corrugated surface?
8.6. What is DPS? What does it attempt to do? What is the difference between DPS and DSW?
8.7. What are the differences between DPS and the HELS method using the DPS expansion?
8.8. What are the optimal regularization schemes for the HELS method using LSW, DSW, and DPS expansions?
8.9. What are the performances of the HELS method using LSW, DSW, and DPS expansions?
8.10. What are the impacts of various parameters such as the locations of the auxiliary sources, number of measurement points, and choices of regularization schemes on the performances of the HELS method using LSW, DSW, and DPS expansions?